Boundary condition

$$
\left.
\begin{aligned}
&z=0,\ \theta=\text{const.}\\
&z=H,\ \frac{\partial\theta}{\partial z}=\alpha(\theta-\theta_a)\\
&r=r_b,\ \frac{\partial\theta}{\partial r}=0\\
&r=r_o,\ (H-l)\leqq z\leqq(H-l+l_e),\quad \theta=\theta_o\\
&r=r_o,\ (H-l+l_e)<z\leqq H,\ \frac{\partial\theta}{\partial r}=0
\end{aligned}
\right\}
\qquad (3)
$$

where θ is the temperature, r the distance from the axis of heat pipe, z the distance from the heat source, τ the time. r_o is the radius of the heat pipe. ρ, c and λ are the density, heat capacity and heat conductivity of the rock. α is the Newton's cooling coefficiency. σ and γ are contant. Subscript a, e and b represent the atomsphere, the evaporator and the boundary.

Equ.(1) with condition (2) and (3) is solved by finite difference method. Calculated values of heat transfer rate are larger than the values obtained from the field experiments. This may be explained as the result of contact resistance on the surface of the evaporator. This result suggests that it should be considered carefully how to minimize the resistance in the further application of heat pipe.

REFERENCE

KIMURA, S., YONEYA, M., IKESHOJI, T., SHIRAISHI, M., (1987): Heat Transfer to Ultra-large-scale Heat Pipes Placed in a Geothermal Reservoir. J. Gerthermal Research Soc. Japan. Vol.9, No.1, 19-30(In Japanese).

KIMURA, S., YONEYA, M., IKESHOJI, T., SHIRAISHI, M., (1988a): Heat Transfer to Ultra-large-scale Heat Pipes Placed in a Geothermal Reservoir - (2nd Report): Transverse Flows. J. Gerthermal Research Soc. Japan. Vol.10, No.1, 51-58(In Japanese).

KIMURA, S., YONEYA, M., IKESHOJI, T., SHIRAISHI, M., (1988b): Heat Transfer to Ultra-large-scale Heat Pipes Placed in a Geothermal Reservoir - (3rd Report): Effects of Natural Convection. J. Gerthermal Research Soc. Japan. Vol.10, No.2, 89-107(In Japanese).

NEJAT,(1981): Int. J. Multiphase Flow. P.321.

SHIRAISHI, M., (1987): Extraction of Geothermal Energy Utilizing Super-scaled Heat Pipes. Geothermics. Vol.24, No.1, 52-62(In Japanese).

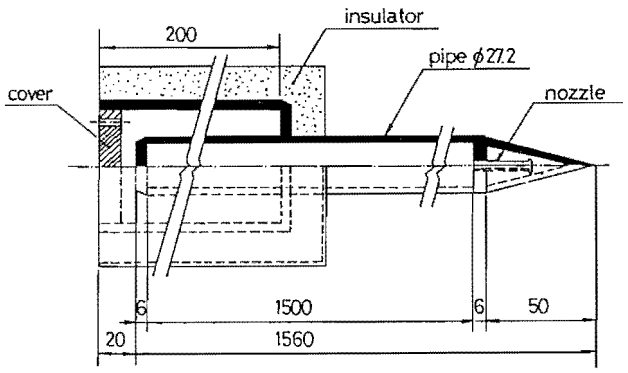

Fig.1 Heat pipe used in the experiments

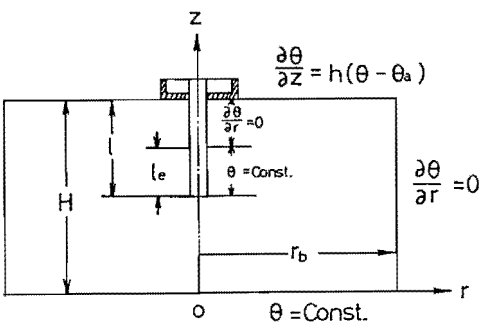

Fig. 2 Analysis modle

VOLCANIC HISTORY AT THE MATSUKAWA-KAKKONDA AREA, NORTHEAST JAPAN

SUTO, S., Geol. Surv. of Japan, Higashi 1-1-3, Tsukuba 305, Japan
ITAYA, T., Hiruzen Research Institute, Okayama Univ. of Sci., 1-1, Ridai-cho, Okayama, 700, Japan
MUKOYAMA, S., Kokusai Aerial Surveys Co., Ltd., Asahigaoka, 3-6-1, Hino, Tokyo 191 Japan

The Matsukawa-Kakkonda area in the central part of the Sengan geothermal area is one of the most active geothermal fields in Japan (Fig. 1). Matsukawa geothermal power station (22,000 kw) in the northeast corner and Kakkonda geothermal power station (50,000 kw) in the southwest corner of the studied area have been operated since 1966 and 1978 respectively.

Outline of geology

Siliceous rock with black and white bands of possible Pre-Neogene was found about 1,550 m below sea level at the borehole for exploiting geothermal resources on the southern flank of Iwate Volcano (Suto and Ishii, 1987). However, no Pre-Neogene has been observed at outcrop in this area. The Koshitomaezawa Formation, Yamatsuda Formation, Kakkonda Pyroclastic Rocks and the Kantonosawa Formation compose the Neogene of this area (Fig. 2). They are composed of sand, silt and tuff. The total thickness of the Miocene sediment is estimated to be more than 1600 m in the Kakkonda area (Nakamura and Sumi, 1981).

The Tamagawa Welded Tuffs are distributed in the wide area of the Sengan area. They are not exposed in the studied area. The Tamagawa Welded Tuffs are divided into the Rhyolite Welded Tuff 4 (R4) and the Dacite Welded Tuff (D) which were erupted in 2 Ma and 1 Ma respectively. The volume of the sediment of these two units are estimated to be 130 km^3 for R4 and 50 km^3 for D (Suto, 1987). It is thought that the large magma reservoir of felsic composition may play some part of the heat source in the Sengan area.

The products of the "Young Volcanoes", mainly andesite composition, in the Sengan area were divided into the Early stage volcanics (erupted in Matsuyama reversed epoch or much older epoch) and the Late stage volcanics (erupted in Brunhes normal epoch)(Suto, 1985; Suto and Mukoyama, 1987). Topographic map with names of the volcanoes is shown in Fig. 3.

Matsukawa Andesite lies directly on the Miocene sediments and is covered by Omatsukurayama, Mitsuishiyama and Iwate Volcanoes. Iwate Volcano is one of the active volcanoes in the Sengan geothermal area, and the eruption center is east of the studied area. All of the young volcanic rocks in the studied area are andesite (Table 1), except those of Iwate Volcano. The volcanic rocks from Mitsuishiyama and Omatsukurayama volcanoes belong to the tholeiitic rock series and those from Matsukawa Andesite, Obukadake and Iwate-Ojiromori Volcanoes belong to the calc-alkali rock series (Fig. 4).

Paleomagnetic study

Samples for paleomagnetic analysis were collected from 23 sites. Localities of each site are shown in Fig. 2. From one to four oriented handsamples were taken from the outcrop. In a

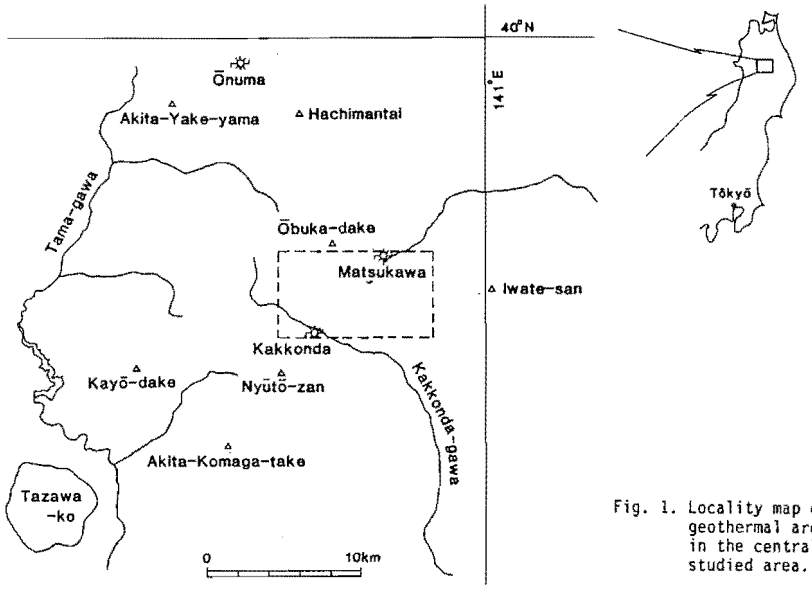

Fig. 1. Locality map of the Sengan geothermal area. The quadrangle in the central part shows the studied area.

laboratory, 2.54 cm diameter core specimens were drilled from the block samples. The intensity and direction of magnetization were measured, employing an astatic magnetometer with a sensitivity of about 1 x 10^{-2} A/m. The demagnetization was performed in an AC field between 10 and 50 mT in a μ metal shield. Initially, one pilot specimen from each site was selected for stepwise demagnetization to choose the height of AC peak field enough for magnetic cleaning. Next, the other specimens of the site were demagnetized in the determined level site by site. Specimens, for which the demagnetization curves and the remanent directions were not stable through the way, were omitted from the final analysis.

The results are shown in Table 2. The direction of magnetization of volcanic rocks of each volcanoes are as follows; Matsukawa Andesite: both normal and reversed, Obukadake and Iwate-

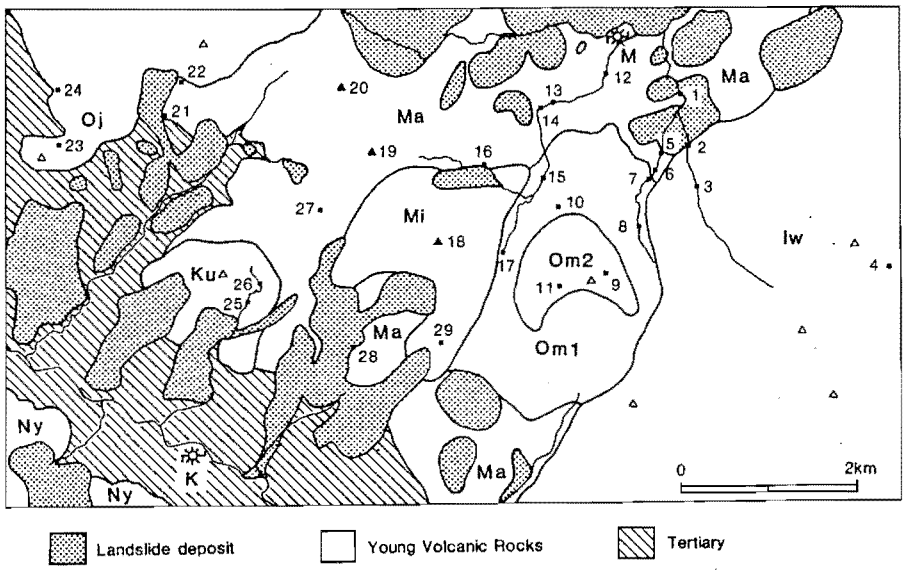

Fig. 2. Geological map of the Matsukawa-Kakkonda area. M : Matsukawa geothermal power station, K : Kakkonda geothermal power station. Ma : Matsukawa andesite, Oj : Obukadake and Iwate-Ojiromori volcano, Om1 : Omatsukurayama lower lava, Om2 : Omatsukurayama volcano, Ku : Kurikigahara volcano, Mi : Mitsuishiyama volcano, Ny : Nyutozan volcano.

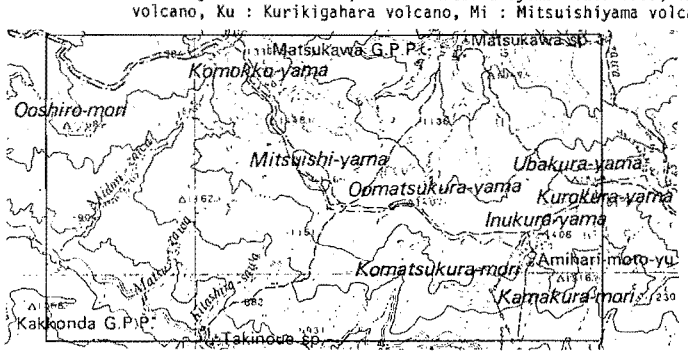

Fig. 3. Topographic map of the Matsukawa -Kakkonda area.

Table 1. Chemical composition of the volcanic rocks.

Loc. No.*	19	21	16	20	24	23	17	10	11	29
No. of specimen	1886	AZ10	MT4	1887	KI16	KI12	MT3	52-16	3-42	2-107
SiO_2	56.70	57.18	60.58	63.18	61.42	63.89	48.73	56.06	58.15	57.27
TiO_2	0.66	0.64	0.68	0.65	0.64	0.55	0.83	0.71	0.99	0.81
Al_2O_3	16.51	16.27	15.17	14.90	15.93	15.19	18.94	17.21	15.69	16.51
Fe_2O_3	2.56	2.62	2.87	3.47	3.71	2.77	4.70	2.27	3.47	3.70
FeO	5.49	4.97	4.47	2.88	2.93	3.11	5.43	6.00	6.55	5.25
MnO	0.15	0.15	0.17	0.11	0.12	0.12	0.18	0.18	0.20	0.18
MgO	4.83	4.25	3.73	2.70	2.89	2.67	5.77	4.91	3.33	3.98
CaO	8.51	8.01	6.84	5.57	4.82	5.70	7.53	8.52	7.34	7.94
Na_2O	2.29	2.27	2.59	2.99	2.55	2.97	1.56	2.63	2.97	2.60
K_2O	0.75	0.80	1.16	1.48	1.17	1.45	0.09	0.52	0.56	0.58
P_2O_5	0.07	0.08	0.09	0.10	0.08	0.09	0.08	0.10	0.11	0.10
$H_2O(+)$	0.99	1.18	0.51	1.00	2.03	0.64	2.91	0.31	0.45	0.79
$H_2O(-)$	0.50	1.51	1.14	0.76	1.47	0.53	3.06	0.62	0.22	0.26
Total	100.01	99.93	100.00	99.79	99.76	99.68	99.81	100.04	100.03	99.97

* nos. as same as those in Fig. 2.

Ojiromori: reversed, Omatsukurayama: normal, Kurikigahara: normal and Iwate: normal. These paleomagnetic data are concordant with the results of Suto (1985) and Suto and Mukoyama (1987).

K-Ar dating

The method of sample preparation and analytical procedure is shown by Itaya et al. (1984). The results are shown in Table 3. The large analytical uncertainty of sample MT-3 from locality no. 17 is due to the very low percentage of radiogenic argon.

K-Ar ages of samples from the Matsukawa Andesite are from 1.29 ± 0.15 to 1.67 ± 0.12 Ma, and these age data are concordant with the reversed paleomagnetic data of these samples. But some of the other rock samples from the Matsukawa Andesite show normal magnetic direction, and they are thought to be erupted in the Olduvai normal event or Gauss normal epoch. Sample KI-16 from Obukadake Volcano also shows the age in the Matuyama reversed epoch. K-Ar age of the sample 1885 from the summit of the Mitsuishiyama Volcano is 0.46 ± 0.05 Ma, which is the youngest age data in the studied area.

Conclusion

Volcanic succession of the studied area is shown in Fig. 5. The "Young Volcanoes" in the Sengan geothermal area were divided into the Early stage and the Later stage volcanics. Mitsuishiyama, Iwate, Nyutozan, and maybe Kurikigahara Volcanoes belong to the Late stage volcanics and the rest to the Early stage volcanics in the studied area. The volume of the effusive rock of Mitsuishiyama and Kurikigahara volcanoes are far smaller than those of Iwate Volcano or Matsukawa Andesite. There is no mutual relation between the site of the geothermal power plant and the eruption age of the nearest volcanoes in the sengan geothermal area.

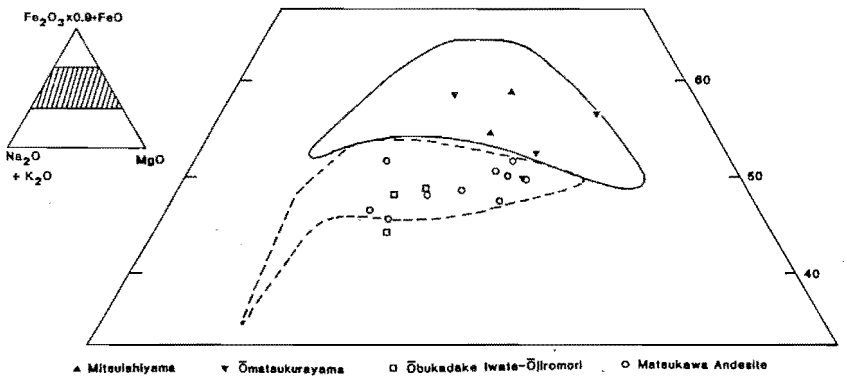

Fig. 4. M-F-A diagram of the volcanic rocks from the Matsukawa-Kakkonda area. Solid line and the broken line show the chemical composition of the tholeiitic rock series and the calc-alkali rock series from the southern part of the Sengan area respectively. Data are quoted from Kawano and Aoki (1960), Suto (1985), Suto and Ishii (1987) and Suto (in prepatation).

Table 2. Paleomagnetic data of the volcanic rocks.

Loc. No.*	No.of specimen	nos.of samples	Cleaning (mT)	Dec.	Inc.	K	α95	Intensity** (10^{-2}A/m)
1	SU1	3	10	352	56	52	17	786
5	OA995	1	20	328	65	-	-	276
6	OA1060	1	20	40	-53	-	-	34
12	MT880	1	10	196	-58	-	-	109
13	MT1	3	40	344	62	401	6	1
14	MT990	1	10	160	-51	-	-	277
16	MT4	3	30	150	-45	14	33	46
21	AZ10	3	20	145	-26	604	5	40
22	AZ11	3	30	184	-52	30	23	3
27	MA3	3	30	192	-50	27	24	2
28	SZ1	3	20	193	-36	35	20	12
23	KI12	3	20	223	-76	29	23	159
24	KI16	3	30	165	-60	189	8	769
7	OA1	3	10	329	53	17	30	601
8	OA115	1	10	7	46	-	-	866
15	MT2	3	20	353	63	99	12	833
17	MT3	3	20	330	59	39	19	803
9	OA2	3	30	343	39	18	29	430
25	MA2	3	10	29	44	83	13	180
26	MA1125	1	10	313	79	-	-	308
2	SU980	1	10	354	36	-	-	310
3	SU1100	1	20	354	61	-	-	413
4	SU2	3	10	5	27	132	10	1300

* nos. as same as those in Fig. 2.
** Intensity before cleaning.